ASPECT RATIO EFFECT IN A THERMALLY-DRIVEN RECTANGULAR OPEN CAVITY WITH AN ISOTHERMAL SHROUDING WALL

Admilson Teixeira Franco - franco@nupes.cefetpr.br
Federal Center for Education in Technology - CEFET - PR
Department of Mechanical Engineering - DAMEC
Thermal Sciences Laboratory - LACIT
Concurrent Engineering R & D Laboratory - NuPES
Av. Sete de Setembro, 3165
80230-901 - Curitiba - PR - Brazil

Marcelo Moreira Ganzarolli - ganza@fem.unicamp.br
State University of Campinas - UNICAMP
Mechanical Engineering Faculty - FEM, Energy Department - DE
Cidade Universitária Zeferino Vaz
13081-970 - Campinas - SP - Brazil

Summary. *Natural convection in a rectangular open cavity with the presence of an isothermal shrouding wall is investigated. The horizontal walls of the cavity are adiabatic. One vertical wall is heated uniformly and another is open to a fluid reservoir. The shrouding wall is placed in front of this opening forming a vertical channel. Laminar and two-dimensional flow is assumed for a Rayleigh number ranging from* $10^3 - 10^7$*. The numerical solution is carried out with the Finite Volume-SOLA method. The aspect ratios considered are* $B = L/H = 0.5$*, 3.0 e 6.0, where* L *and* H *are the cavity width and height, respectively. The Rayleigh number and the aspect ratios effect on the isotherms, streamlines and average Nusselt number are reported.*

Key-words: *Natural convection, Aspect ratio effect, Shrouding wall, Open cavity, SOLA method*

1. INTRODUCTION

The importance of studying natural convection heat transfer in a cavity with electronic components has increased in recent years. Among the advantages of using natural convection in such kind of problems, possibly the most importants are safety, reliability and low cost. Other engineering applications like building insolation and solar cavity receivers have received a lot of attention too.

Reviewing the technical literature, one can find many works studying the problem of a

heated cavity with an opening to a fluid reservoir. One can mention the papers by Penot (1982), Chan e Tien (1985a), Chan e Tien (1985b), Chan e Tien (1986), Humphrey and To (1986), Angirasa *et al.* (1992) and Angirasa *et al.* (1995). All these previous studies did not consider the effects of a shrouding wall. In a recent paper, Franco and Ganzarolli (1998) carried out a numerical study of a thermally driven square open cavity open to a fluid reservoir with and without a shrouding wall.

The present paper has as purpose to investigate the heat transfer phenomenon in a thermally-driven rectangular open cavity as a function of the aspect ratio B and the distance between the opening and the shrouding isothermal wall. One will use an extended computational domain outside of the cavity.

2. PROBLEM FORMULATION

The cavity geometry and the boundary conditions are shown in Fig. 1. The open cavity is the $L \times H$ domain. The extended domain is the region $b \times Z$, where $Z = 5H$. The vertical wall inside the cavity is maintained at constant temperature T_h and the fluid reservoir (or ambient) at T_o. Laminar flow is assumed and the Boussinesq approximation is considered valid. The dimensionless variables are defined below.

$$(X, Y) = \frac{(x, y)}{H}. \tag{1}$$

$$(U, V) = \frac{(u, v)H}{\alpha}. \tag{2}$$

$$\tau = \frac{\alpha t}{H^2}. \tag{3}$$

$$T = \frac{T^\circ - T^\circ_\infty}{(T^\circ_h - T^\circ_\infty)}. \tag{4}$$

$$P = \frac{(p - p_\infty)H^2}{\rho\alpha^2}. \tag{5}$$

where T° indicates the dimensional temperature value.

Using the variables above, one can write the dimensionless conservation equation for mass, momentum and energy in transient form as

$$\frac{\partial U}{\partial X} + \frac{\partial V}{\partial Y} = 0. \tag{6}$$

$$\frac{\partial U}{\partial \tau} + \frac{\partial (U^2)}{\partial X} + \frac{\partial (VU)}{\partial Y} = -\frac{\partial P}{\partial X} + Pr\left(\frac{\partial^2 U}{\partial X^2} + \frac{\partial^2 U}{\partial Y^2}\right). \tag{7}$$

$$\frac{\partial V}{\partial \tau} + \frac{\partial (UV)}{\partial X} + \frac{\partial (V^2)}{\partial Y} = -\frac{\partial P}{\partial Y} + Pr\left(\frac{\partial^2 V}{\partial X^2} + \frac{\partial^2 V}{\partial Y^2}\right) + Ra.Pr.T. \tag{8}$$

$$\frac{\partial T}{\partial \tau} + \frac{\partial (UT)}{\partial X} + \frac{\partial (VT)}{\partial Y} = \left(\frac{\partial^2 T}{\partial X^2} + \frac{\partial^2 T}{\partial Y^2}\right). \tag{9}$$

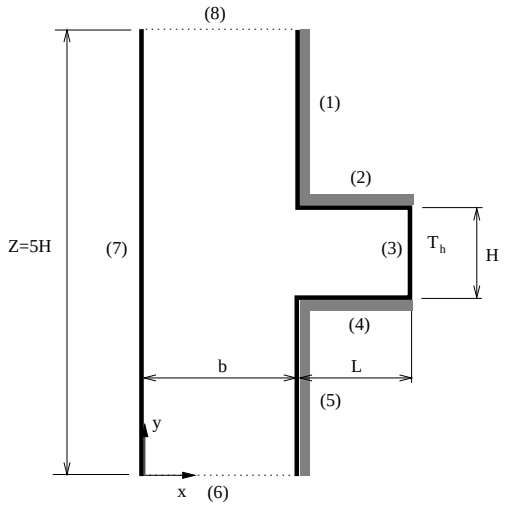

Figure 1: Geometry and the coordinate system

where the quantities $Pr = \nu/\alpha$ and $Ra = g\beta H^3(T_h^\circ - T_\infty^\circ)/\alpha\nu$ are the Prandtl and the Rayleigh numbers, respectively.

The boundary conditions at the borders show in Fig. 1 are

$$(1) \rightarrow U = V = \partial T/\partial X = 0. \tag{10}$$

$$(2) \rightarrow U = V = \partial T/\partial Y = 0. \tag{11}$$

$$(3) \rightarrow U = V = 0eT = 1. \tag{12}$$

$$(4) \rightarrow U = V = \partial T/\partial Y = 0. \tag{13}$$

$$(5) \rightarrow U = V = \partial T/\partial X = 0. \tag{14}$$

$$(6) \rightarrow (\partial U/\partial Y) = (\partial V/\partial Y) = (\partial T/\partial Y)_{out} = 0 \quad \text{and} \quad T_{in} = 0. \tag{15}$$

$$(7) \rightarrow U = V = 0 \quad \text{and} \quad T = 0. \tag{16}$$

$$(8) \rightarrow (\partial U/\partial Y) = (\partial V/\partial Y) = (\partial T/\partial Y)_{out} = 0 \quad \text{and} \quad T_{in} = 0. \tag{17}$$

The average Nusselt number on the heated wall, $\overline{Nu}$, is defined as

$$\overline{Nu} = \int_0^1 \left(\frac{\partial T}{\partial X}\right)_{X=0} dY = \overline{Nu}(Ra, Pr, B). \tag{18}$$

The dimensionless stream function is

$$\Psi(X,Y) = -\int_{X_o}^{X} V(X,Y)dX + \Psi(X_o, Y_o). \tag{19}$$

where the value $\Psi(X_o, Y_o)$ is zero in the solid walls.

The dimensionless volumetric flow rate is defined as

$$\dot{m} = \int_{Opening} U_{in} dY. \tag{20}$$

$$U_{in} = U_{X=b/H} \quad \text{if} \quad U_{X=b/H} > 0$$
$$U_{in} = 0 \quad \text{if} \quad U_{X=b/H} \leq 0$$

3. NUMERICAL PROCEDURE

The equations above were solved with the Finite Volume Method (Patankar, 1980) for spatial discretization and the SOLA method for time discretization (Hirt *et al.* (1975)). The SOLA method consists of advancing in time the velocity and pressure fields from a previous values of velocities, stopping the procedure when convergence criteria is reached

$$\max \left| \frac{\phi^{n+1} - \phi^n}{\phi^{n+1}} \right| < 10^{-5}. \tag{21}$$

where $\phi = U, V, T$ and Nu.

The numerical code was validated by checking this with the Chan and Tien (1985b) results. For example, at $Ra = 10^6$ and using 21×21 points inside the cavity, the values obtained for $\overline{Nu}$ and $\dot{m}$ are 15.0 and 47.3 against 15.0 and 47.6 obtained by Chan and Tien (1985b).

For an aspect ratio like B =1.0 and $Ra = 10^5$, when the points inside the cavity are increased from 21×21 to 31×31, the verage Nusselt number variation is less than 0.2%.

4. RESULTS AND DISCUSSION

In this section is solved the natural convection problem schematically showed in Fig. 1.

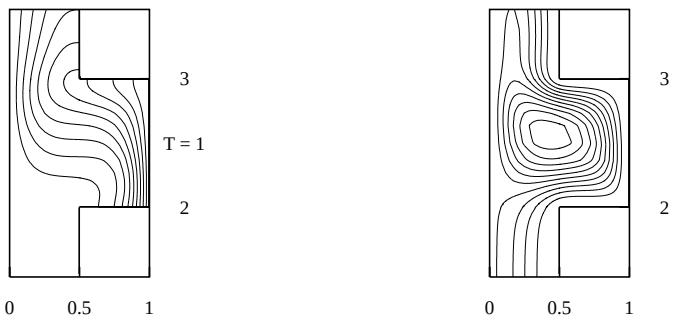

a-) b/H=0.5 e $|\Delta\Psi|$=0,600

b-) b/H=0.2 e $|\Delta\Psi|$=0,400

Figure 2: Isothermals and streamlines for $Ra = 10^4$ and $B = 0.5$

The cavity aspect ratios considered are $B = L/H$ =0.5, 3.0 and 6.0 for a Rayleigh number ranging from $Ra = 10^3 - 10^7$. The distance between the opening and the shrouding wall, b/H, is considered as 0.5 and 0.2. The Prandtl number is set at 1.0, which is approximately air.

In the following figures, the contour maps showing the isotherms and the streamlines are plotted. The intervals between the isotherms are always $\Delta T = 0.1$ and for the streamlines it is shown together with each figure. Only the region near the open cavity is shown in order to save space.

Figure 2 shows for a $Ra = 10^4$, the isothermals and streamlines patterns when the isothermal shrouding wall approximates to the opening of the cavity. In this case the aspect ratio diminishes from b/H =0.5 to 0.2.

The effect of reducing de distance b/H, in Figs. 2, 3 and 4 is to limit the recirculation zone into the cavity. When b/H is 0.2, the isothermals and streamlines are similar of that cavity heated on the sides (Hortman *et al.* (1990) and Lé Quére (1991)).

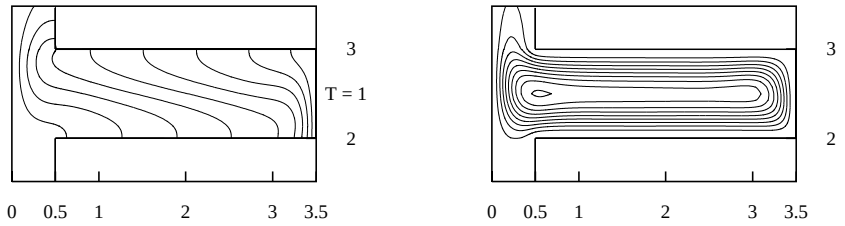

a-) b/H=0.5 e $|\Delta\Psi|$=0.500

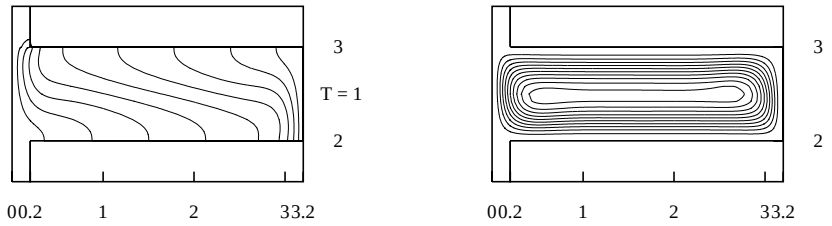

b-) b/H=0.2 e $|\Delta\Psi|$=0,400

Figure 3: Isothermals and streamlines for $Ra = 10^4$ and $B = 3.0$

When the cavity becomes deeper, the isotherms are distributed along the cavity, diminishing the temperature gradient between the heated and the isothermal wall.

Figure 5 presents the dimensionless mass flow rate $\dot{M}$, which is induced by the heated wall into the channel through the bottom boundary. One can see that for $b/H = 0.5$ the channel flow appears at $Ra \cong 10^4$. The channel flow is presented for $b/H = 0.2$ just when the Rayleigh number is around or bigger than 10^5. In this section, the behavior of the curves are practically the same. shrouding

Figure 6, for $Ra = 10^3$, shows the isotherms for the situation when the dominant heat transfer mechanism is the conduction. The temperature gradient is practically the same in both cases.

The boundary layer regime is shown in Fig. 7 for $Ra = 10^6$. Just the isothermals are

presented. For all aspect ratios B, when the isothermal shrouding wall gets closer of the opening, the temperature gradient becomes higher on the heated wall.

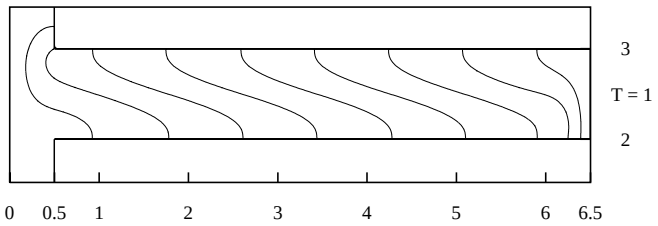

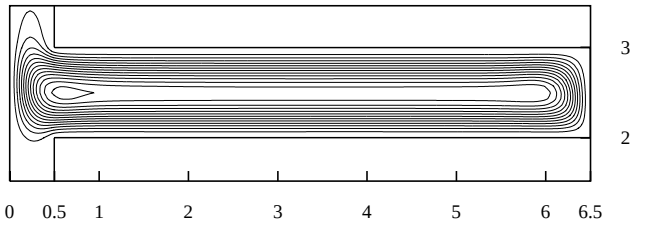

a-) b/H=0.5 e $|\Delta\Psi|$=0.250

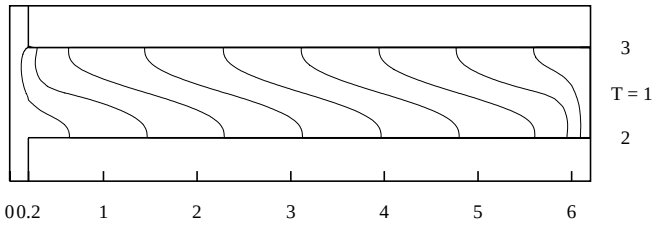

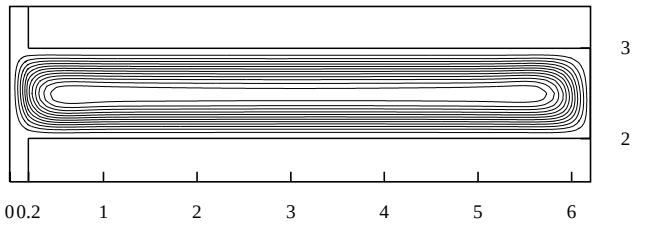

b-) b/H=0.2 e $|\Delta\Psi|$=0.250

Figure 4: Isothermals and streamlines for $Ra = 10^4$ and $B = 6.0$

From a thermal engineering point of view, one of the most important parameters is the average Nusselt number on the heated wall. The average Nusselt number as a function of the Rayleigh number is shown in the Fig. 8.

At $Ra = 10^3$, considering that the conduction heat transfer mechanism is dominant, the average Nusselt number is determined as

$$\overline{Nu} \cong \frac{h.H}{k} \cong \frac{H}{L} = (B)^{-1}. \tag{22}$$

where h is determined as a function of the total heat transfer $Q = h.H.\Delta T^{\circ}$

$$Q \cong k.H.\frac{\Delta T^{\circ}}{L}.$$

where $h \cong k/L$. Equation (22), provides the following values for the average Nusselt number: 2.000, 0.333 e 0.167 for B =0.5, 3.0 e 6.0, respectively.

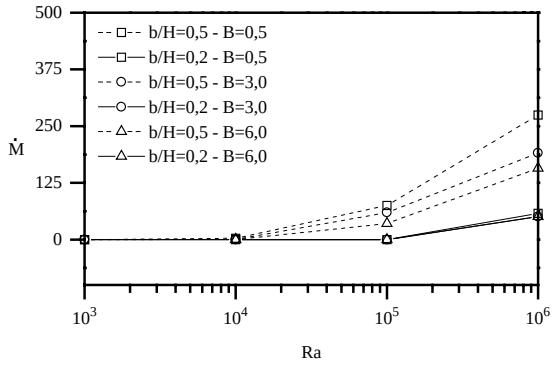

Figure 5: Volumetric mass flow (rate) $\dot{M}$ entering in the channel

As it was pointed by Chan e Tien (1985a), the average Nusselt number approaches its value for the vertical wall in an infinite medium. The average Nusselt number is expressed by

$$\overline{Nu} \cong Ra^{1/4}. \tag{23}$$

which is the power-law for a vertical boundary layer generates by natural convection.

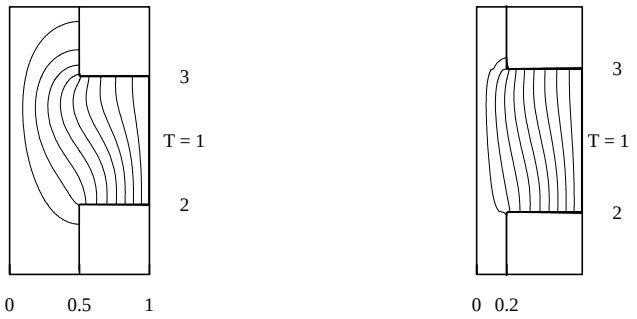

a-) b/H=0.5 e 0.2 - B=0.5

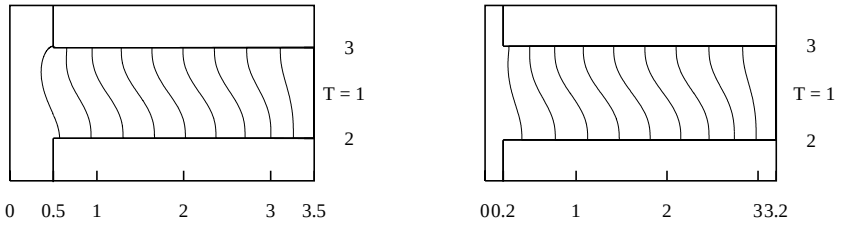

b-) b/H=0.5 e 0.2 - B=3.0

Figure 6: Isothermals for the conduction limit and $Ra = 10^3$

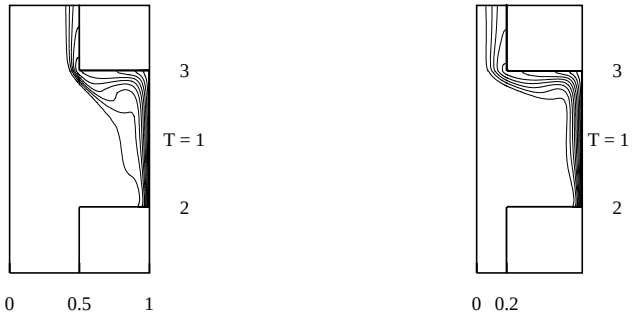

a-) b/H=0.5 e 0.2 - B=0.5

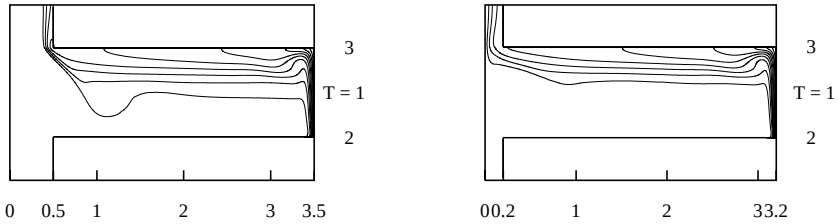

b-) b/H=0.5 e 0.2 - B=3.0

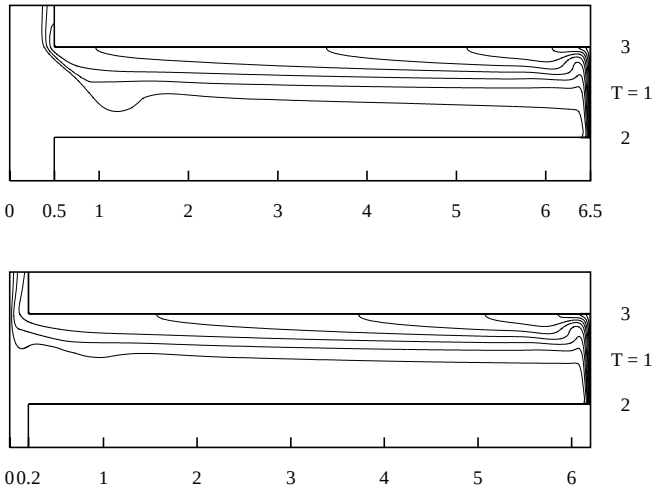

c-) b/H=0.5 e 0.2 - B=6.0

Figure 7: Isothermals for the boundary layer regime and $Ra = 10^6$

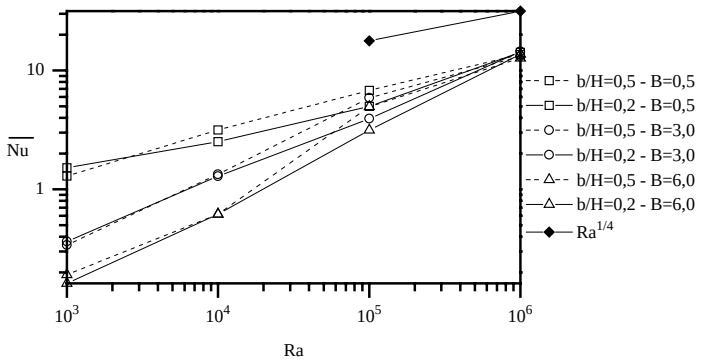

Figure 8: Rayleigh number effect on the average Nusselt number

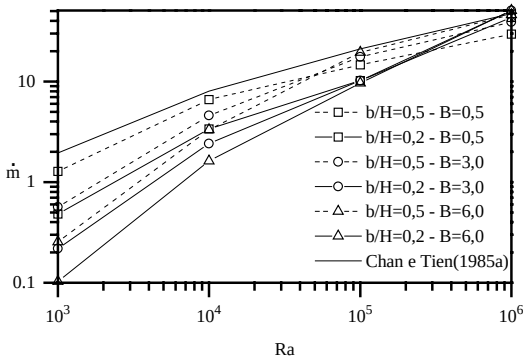

Figure 9: Aspect ratio effect on the volumetric flow rate $\dot{m}$

Figure 9 illustrates the volumetric flow rate, $\dot{m}$, induced through the cavity by the heated wall. The Chan and Tien (1985a) results are plotted for comparison and they are valid when there is not the presence of the shrouding wall. It is noted that there is a change in the curve slope for $b/H = 0.5$ and $Ra \cong 4.5 \times 10^4$.

5. CONCLUDING REMARKS

In this work was studied the aspect ratio effect in a thermally-driven rectangular open cavity with an isothermal shrouding wall. The aspect ratios considered were $B = L/H =$ 0.5, 3.0 and 6.0 and the horizontal distance between the shrouding and the opening was done as b/H=0.2 and 0.5.

The limit when b/H (which is the distance between the opening and the shrouding isothermal wall) tends to zero, becomes the patterns of the isothermals and streamlines similar to the classical problem of the closed cavity heated on the sides.

For b/H=0.5, when the Rayleigh number is around 10^5 or bigger, the channel flow appears. Otherwise, when Rayleigh is little than this value, the flow is restricted into the cavity. For b/H=0.2, the channel flow appears just when $Ra \geq 10^6$.

At low Rayleigh numbers, little than 10^3, the Nusselt number can be evaluated as $Nu \cong (B)^{-1}$, Equation (22), the inverse of the aspect ratio $B = L/H$. At high values of the Rayleigh number, the results tend asymptotically for that of a natural convection boundary layer in a vertical flat plate, $Nu \cong Ra^{1/4}$, Equation (23).

The volumetric flow rate $\dot{m}$, induced into the cavity by the heated wall, for b/H=0.5, changes the slope at $Ra \geq 4.5 \times 10^4$. After that point, the deeper cavity induces more $\dot{m}$ through the cavity. The behavior of the curves are analogous for b/H=0.2.

6. REFERENCES

Angirasa, D., Eggels, J. E. M. and Niewstadt, F. T. M., 1995, Numerical Simulation of Transient Natural Convection from an Isothermal Cavity Open on a Side, *Numerical Heat Transfer*, Vol. 28, Part A, pp. 755-768.

Angirasa, D., Pourquié, M. J. B. M. and Niewstadt, F. T. M., 1992, Numerical Study of Transient and Steady Laminar Buoyancy-Driven Flows and Heat Transfer in a Square Open Cavity, *Numerical Heat Transfer*, Vol. 22, Part A, pp. 223-239.

Bejan, A., 1993, *Heat Transfer*, John Wiley & Sons, USA.

Bejan, A., 1994, *Convection Heat Transfer*, John Wiley & Sons, 2ª edição , USA.

Chan, Y. L. and Tien, C. L., 1985a, A Numerical Study of Two-Dimensional Natural Convection in a Square Open Cavities, *Numerical Heat Transfer*, Vol. 8, pp. 65-80.

Chan, Y. L. and Tien, C. L., 1985b, A Numerical Study of Two-Dimensional Laminar Natural Convection in a Shallow Open Cavities, *International Journal Heat Mass Transfer*, Vol. 28, nº 3, pp. 603-612.

Chan, Y. L. and Tien, C. L., 1986, Laminar Natural Convection in a Shallow Open Cavities, *Journal of Heat Transfer*, Vol. 108, pp. 305-309.

Franco, A. T. and Ganzarolli, M. M., 1998, Numerical Study of a Thermally-Driven Open Cavity With and Without a Shrouding Wall, *Proceedings of the VII ENCIT*, November 03-06, Rio de Janeiro, Vol. 1, pp. 207-212.

Hirt, C. W., Nichols, B.D. and Romero, N.C., 1975, SOLA- Numerical Solution Algorithm for Transient Fluid Flow, *Los Alamos Laboratory*, Report LA-5852.

Hortmann, M., Peric, M. and Scheuerer, G., 1990, Finite Volume Multigrid Prediction of Laminar Natural Convection: Bench Mark Solution, *International Journal for Numerical Methods in Fluids*, Vol. 11, pp. 189-207.

Lé Quére, P., 1991, Accurate Solutions to the Square Thermally Driven Cavity at High Rayleigh Number, *Computer Fluids*, Vol. 20, nº 1, pp. 29-41.

Patankar, S. V., 1980, *Numerical Heat Transfer and Fluid Flow*, Hemisphere Publishing Corporation, USA.